Sliding Window Decoding of LDPC Convolutional Codes

Daniel J. Costello, Jr.[1]

Joint work with Min Zhu[2], David G. M. Mitchell[3], and Michael Lentmaier[4]

Workshop on Convolutional Codes, Zurich, Switzerland, June 5, 2023

[1] Dept. of Electrical Engineering, University of Notre Dame, IN, USA

[2] State Key Lab. of ISN, Xidian University, Xi'an, China

[3] Dept. of Electrical and Computer Engineering, New Mexico State University, NM, USA

[4] Dept. of Electrical and Information Technology, Lund University, Lund, Sweden

Outline

Introduction

- LDPC *Convolutional* codes, also known as *spatially coupled* LDPC (SC-LDPC) codes, are promising candidates for next generation communication systems as a result of the *threshold saturation effect*, whereby they can approach capacity performance with low complexity *belief propagation* (BP) decoding [1, 2].

[1] M. Lentmaier, A. Sridharan, D. J. Costello, Jr., and K. Sh. Zigangirov, "Iterative decoding threshold analysis for LDPC convolutional codes," *IEEE Trans. Inf. Theory*, vol. 56, no. 10, pp. 5274-5289, Oct. 2010.
[2] S. Kudekar, T. J. Richardson, and R. L. Urbanke, "Threshold saturation via spatial coupling: Why convolutional LDPC ensembles perform so well over the BEC," *IEEE Trans. Inf. Theory*, vol. 57, no. 2, pp. 803-834, Feb. 2011.
[3] K. Huang, D. G. M. Mitchell, L. Wei, X. Ma, and D. J. Costello, Jr., "Performance comparison of LDPC block and spatially coupled codes over GF(q)," *IEEE Trans. Commun.*, vol. 63, no. 3, pp. 592-604, Mar. 2015.

Introduction

- LDPC *Convolutional* codes, also known as *spatially coupled* LDPC (SC-LDPC) codes, are promising candidates for next generation communication systems as a result of the *threshold saturation effect*, whereby they can approach capacity performance with low complexity *belief propagation* (BP) decoding [1, 2].
- *Near capacity performance* has been demonstrated for large *frame lengths* L, and significantly improved performance compared to LDPC block codes (LDPC-BCs) can be achieved with similar decoding latency, memory, and complexity by using *sliding window decoding* (SWD).

[1] M. Lentmaier, A. Sridharan, D. J. Costello, Jr., and K. Sh. Zigangirov, "Iterative decoding threshold analysis for LDPC convolutional codes," *IEEE Trans. Inf. Theory*, vol. 56, no. 10, pp. 5274-5289, Oct. 2010.
[2] S. Kudekar, T. J. Richardson, and R. L. Urbanke, "Threshold saturation via spatial coupling: Why convolutional LDPC ensembles perform so well over the BEC," *IEEE Trans. Inf. Theory*, vol. 57, no. 2, pp. 803-834, Feb. 2011.
[3] K. Huang, D. G. M. Mitchell, L. Wei, X. Ma, and D. J. Costello, Jr., "Performance comparison of LDPC block and spatially coupled codes over GF(q)," *IEEE Trans. Commun.*, vol. 63, no. 3, pp. 592-604, Mar. 2015.

Introduction

- LDPC *Convolutional* codes, also known as *spatially coupled* LDPC (SC-LDPC) codes, are promising candidates for next generation communication systems as a result of the *threshold saturation effect*, whereby they can approach capacity performance with low complexity *belief propagation* (BP) decoding [1, 2].
- *Near capacity performance* has been demonstrated for large *frame lengths* L, and significantly improved performance compared to LDPC block codes (LDPC-BCs) can be achieved with similar decoding latency, memory, and complexity by using *sliding window decoding* (SWD).
- For SWD of SC-LDPC codes, near capacity performance typically requires a window size $W \geq 6\eta$, where η represents the *decoding constraint length* [3].

[1] M. Lentmaier, A. Sridharan, D. J. Costello, Jr., and K. Sh. Zigangirov, "Iterative decoding threshold analysis for LDPC convolutional codes," *IEEE Trans. Inf. Theory*, vol. 56, no. 10, pp. 5274-5289, Oct. 2010.
[2] S. Kudekar, T. J. Richardson, and R. L. Urbanke, "Threshold saturation via spatial coupling: Why convolutional LDPC ensembles perform so well over the BEC," *IEEE Trans. Inf. Theory*, vol. 57, no. 2, pp. 803-834, Feb. 2011.
[3] K. Huang, D. G. M. Mitchell, L. Wei, X. Ma, and D. J. Costello, Jr., "Performance comparison of LDPC block and spatially coupled codes over GF(q)," *IEEE Trans. Commun.*, vol. 63, no. 3, pp. 592-604, Mar. 2015.

Introduction

- *Challenge with SWD*: for low latency (small decoder window size W) and/or near capacity signal-to-noise ratio (SNR) operation, *decoder error propagation* can occasionally result, causing significant performance degradation.

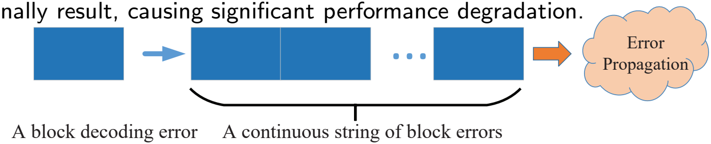

[4] K. Klaiber, S. Cammerer, L. Schmalen, and S. t. Brink, "Avoiding burstlike error patterns in windowed decoding of spatially coupled LDPC codes," in *Proc. IEEE 10th Int. Symp. on Turbo Codes & Iterative Inf. Processing* (ISTC), Hong Kong, China, 2018, pp. 1-5.
[5] M. Zhu, D. G. M. Mitchell, M. Lentmaier, D. J. Costello, Jr., and B. Bai, "Combating error propagation in window decoding of braided convolutional codes," in *Proc. IEEE Int. Symp. Information Theory* (ISIT), Vail, CO, USA, June 17-22, 2018, pp. 1380-1384.
[6] S. ten Brink, "Rate one-half code for approaching the Shannon limit by 0.1 dB," *Electronics Letters*, vol. 36, no. 15, pp. 1-2, Jul. 20, 2000.

Introduction

- *Challenge with SWD*: for low latency (small decoder window size W) and/or near capacity signal-to-noise ratio (SNR) operation, *decoder error propagation* can occasionally result, causing significant performance degradation.

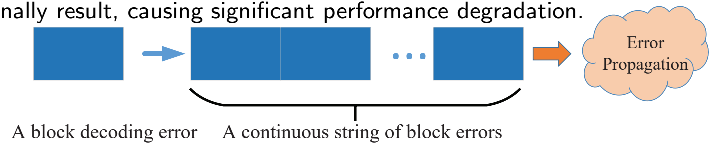

- This effect is particularly harmful and can be catastrophic for large L or continuous (streaming) transmission.

[4] K. Klaiber, S. Cammerer, L. Schmalen, and S. t. Brink, "Avoiding burstlike error patterns in windowed decoding of spatially coupled LDPC codes," in *Proc. IEEE 10th Int. Symp. on Turbo Codes & Iterative Inf. Processing* (ISTC), Hong Kong, China, 2018, pp. 1-5.
[5] M. Zhu, D. G. M. Mitchell, M. Lentmaier, D. J. Costello, Jr., and B. Bai, "Combating error propagation in window decoding of braided convolutional codes," in *Proc. IEEE Int. Symp. Information Theory* (ISIT), Vail, CO, USA, June 17-22, 2018, pp. 1380-1384.
[6] S. ten Brink, "Rate one-half code for approaching the Shannon limit by 0.1 dB," *Electronics Letters*, vol. 36, no. 15, pp. 1-2, Jul. 20, 2000.

Introduction

- *Challenge with SWD*: for low latency (small decoder window size W) and/or near capacity signal-to-noise ratio (SNR) operation, *decoder error propagation* can occasionally result, causing significant performance degradation.

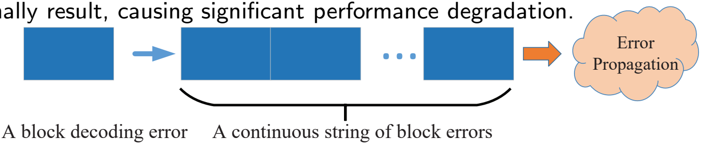

- This effect is particularly harmful and can be catastrophic for large L or continuous (streaming) transmission.
- Related works:
  $\rightarrow$ Klaiber et al. proposed adapting the number of decoder iterations and shifting the window position to combat the error propagation [4].
  $\rightarrow$ Zhu et al. proposed error propagation mitigation techniques for braided convolutional codes with SWD [5].

[4] K. Klaiber, S. Cammerer, L. Schmalen, and S. t. Brink, "Avoiding burstlike error patterns in windowed decoding of spatially coupled LDPC codes," in *Proc. IEEE 10th Int. Symp. on Turbo Codes & Iterative Inf. Processing* (ISTC), Hong Kong, China, 2018, pp. 1-5.
[5] M. Zhu, D. G. M. Mitchell, M. Lentmaier, D. J. Costello, Jr., and B. Bai, "Combating error propagation in window decoding of braided convolutional codes," in *Proc. IEEE Int. Symp. Information Theory* (ISIT), Vail, CO, USA, June 17-22, 2018, pp. 1380-1384.
[6] S. ten Brink, "Rate one-half code for approaching the Shannon limit by 0.1 dB," *Electronics Letters*, vol. 36, no. 15, pp. 1-2, Jul. 20, 2000.

Introduction

- *Challenge with SWD*: for low latency (small decoder window size W) and/or near capacity signal-to-noise ratio (SNR) operation, *decoder error propagation* can occasionally result, causing significant performance degradation.

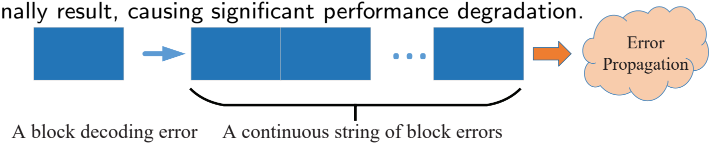

- This effect is particularly harmful and can be catastrophic for large L or continuous (streaming) transmission.
- Related works:
  $\rightarrow$ Klaiber et al. proposed adapting the number of decoder iterations and shifting the window position to combat the error propagation [4].
  $\rightarrow$ Zhu et al. proposed error propagation mitigation techniques for braided convolutional codes with SWD [5].
- We now present several *code doping* techniques that can be used to mitigate the effects of error propagation in SWD. (The concept of code doping was first introduced in a different context by ten Brink [6].)

[4] K. Klaiber, S. Cammerer, L. Schmalen, and S. t. Brink, "Avoiding burstlike error patterns in windowed decoding of spatially coupled LDPC codes," in *Proc. IEEE 10th Int. Symp. on Turbo Codes & Iterative Inf. Processing* (ISTC), Hong Kong, China, 2018, pp. 1-5.
[5] M. Zhu, D. G. M. Mitchell, M. Lentmaier, D. J. Costello, Jr., and B. Bai, "Combating error propagation in window decoding of braided convolutional codes," in *Proc. IEEE Int. Symp. Information Theory* (ISIT), Vail, CO, USA, June 17-22, 2018, pp. 1380-1384.
[6] S. ten Brink, "Rate one-half code for approaching the Shannon limit by 0.1 dB," *Electronics Letters*, vol. 36, no. 15, pp. 1-2, Jul. 20, 2000.

LDPC Block Code Protographs

Parity-check matrix view

- (3,4)-regular

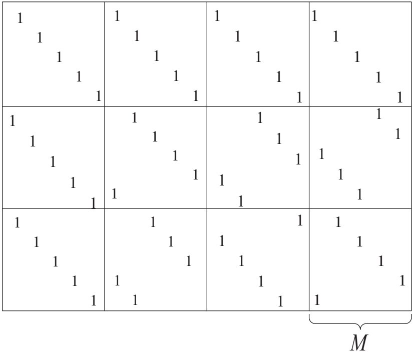

Protograph view

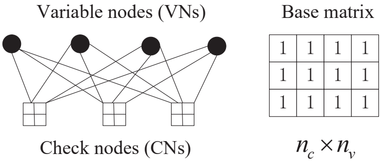

- "Lifting factor" M
- 1 protograph node $= M$ Tanner graph nodes
- 1 protograph edge $= M$ Tanner graph edges

Spatially Coupled LDPC (SC-LDPC) Code Protographs

- Consider the transmission of independent (3,6)-regular blocks over time from an LDPC-BC with (1×2) base matrix $\mathbf{B} = [3\ 3]$, where each block contains $n_v M = 2M$ code symbols.

Spatially Coupled LDPC (SC-LDPC) Code Protographs

- Consider the transmission of independent (3,6)-regular blocks over time from an LDPC-BC with (1×2) base matrix $\mathbf{B} = [3\ 3]$, where each block contains $n_v M = 2M$ code symbols.
- To form an SC-LDPC code, blocks are connected by *spreading edges* to their nearest w neighbors (introducing *memory* into the encoding process), where w is the *coupling width* and the *decoding constraint length* is $\eta = 2M(w+1)$.

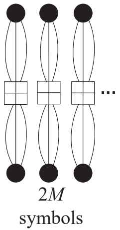

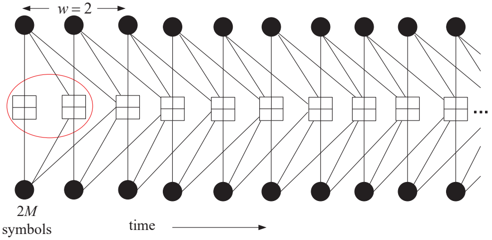

Spatially Coupled LDPC (SC-LDPC) Code Protographs

- To form an SC-LDPC code, blocks are connected by *spreading edges* to their nearest w neighbors (introducing *memory* into the encoding process), where w is the *coupling width* and the *decoding constraint length* is $\eta = 2M(w+1)$.

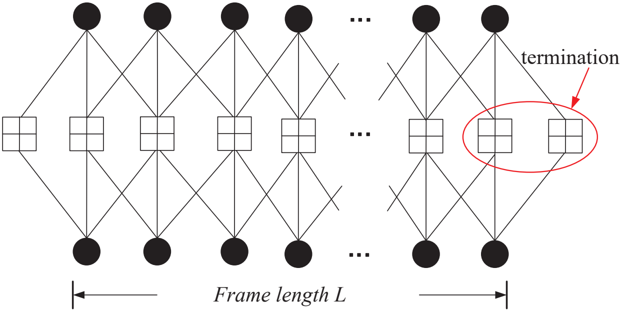

→ When transmission is terminated, the frame length L is defined as the total number of blocks transmitted and BP decoding can be carried out over the entire frame.

Spatially Coupled LDPC (SC-LDPC) Code Protographs

- To form an SC-LDPC code, blocks are connected by *spreading edges* to their nearest w neighbors (introducing *memory* into the encoding process), where w is the *coupling width* and the *decoding constraint length* is $\eta = 2M(w+1)$.

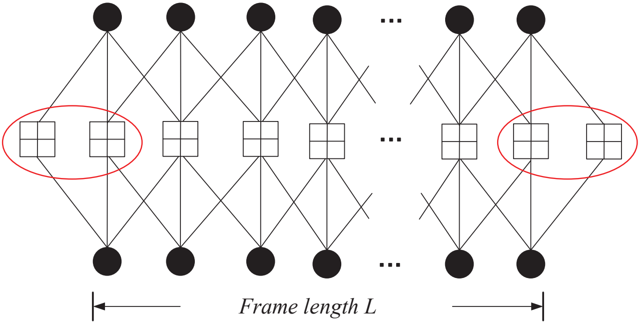

→ The edge spreading results in a *structured irregularity* at both ends of the graph, which triggers *decoding wave propagation*, resulting in *threshold saturation* (BP threshold → MAP threshold) for large M and L.

Spatially Coupled LDPC (SC-LDPC) Code Protographs

- To form an SC-LDPC code, blocks are connected by *spreading edges* to their nearest w neighbors (introducing *memory* into the encoding process), where w is the *coupling width* and the *decoding constraint length* is $\eta = 2M(w+1)$.

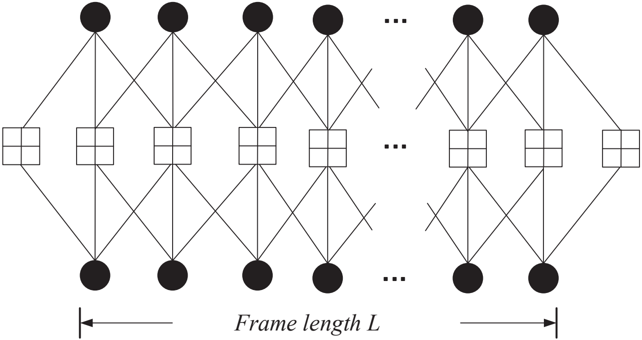

→ SC-LDPC codes combine the best features of regular and irregular LDPC block codes - linear growth of minimum distance with L (regular) and capacity approaching BP thresholds (irregular).

Sliding Window Decoding (SWD) of SC-LDPC Codes

- To form an SC-LDPC code, blocks are connected by *spreading edges* to their nearest w neighbors (introducing *memory* into the encoding process), where w is the *coupling width* and the *decoding constraint length* is $\eta = 2M(w+1)$.

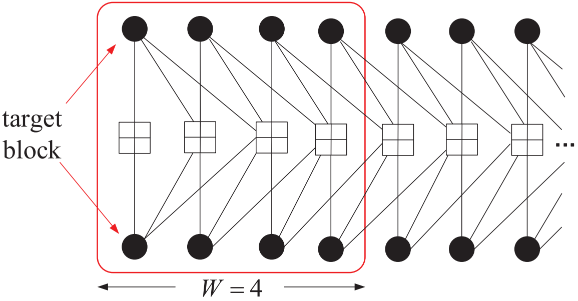

$\rightarrow$ To reduce decoding latency, decoding of a *target block* is jointly carried out over a *window* of size W blocks, where typically $W \ll L$.

Sliding Window Decoding (SWD) of SC-LDPC Codes

- To form an SC-LDPC code, blocks are connected by spreading edges to their nearest w neighbors (introducing memory into the encoding process), where w is the *coupling width* and the *decoding constraint length* is $\eta = 2M(w+1)$.

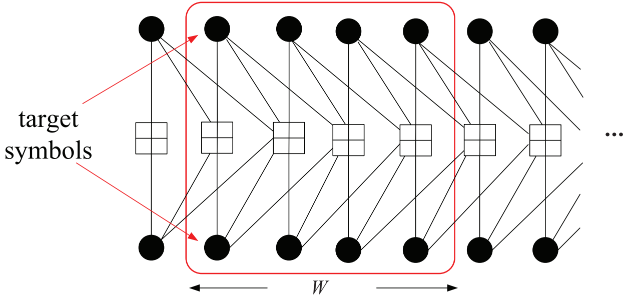

$\rightarrow$ Then the window shifts by one block to decode the next target block.

Sliding Window Decoding (SWD) of SC-LDPC Codes

- To form an SC-LDPC code, blocks are connected by spreading edges to their nearest w neighbors (introducing memory into the encoding process), where w is the *coupling width* and the *decoding constraint length* is $\eta = 2M(w+1)$.

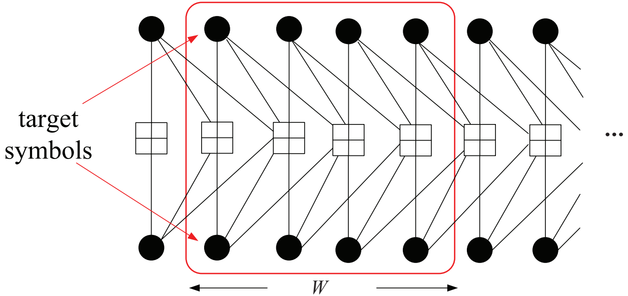

→ Then the window shifts by one block to decode the next target block.
→ For low latency (small W) and/or near capacity (low SNR) operation, decoder error propagation can result.

Cause of Decoder Error Propagation

- The final variable node LLRs from time $t-w+1$ to time t *are used to update* the CNs in the window during the decoding of the target symbols at time $t+1$, although these LLRs are no longer updated, as illustrated in the *spatially coupled base matrix* below:

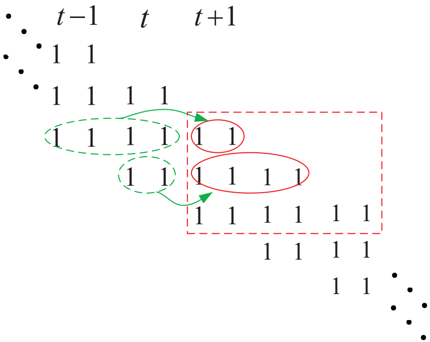

Cause of Decoder Error Propagation

- The final variable node LLRs from time $t - w + 1$ to time t *are used to update* the CNs in the window during the decoding of the target symbols at time $t + 1$, although these LLRs are no longer updated, as illustrated in the *spatially coupled base matrix* below:

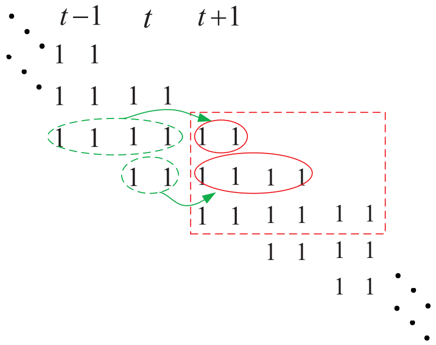

- If an erroneously decoded block contains a high number of incorrect LLRs with large magnitudes, this could trigger additional block errors, resulting in an *error propagation* effect, i. e., a continuous sequence of erroneously decoded blocks.

Effect of Decoder Error Propagation

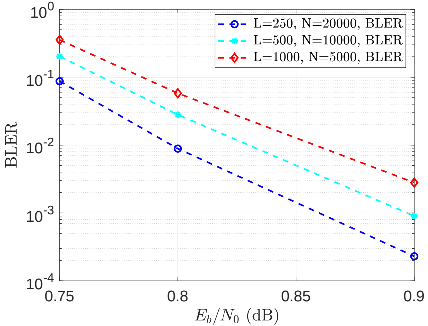

Figure 1: BLER performance of a (3,6)-regular SC-LDPC code for three different combinations of frame length L and number of frames N simulated, all with the same total number of simulated blocks ($LN = 5 \times 10^6$ blocks), for an AWGN channel with BPSK signaling.

Effect of Decoder Error Propagation

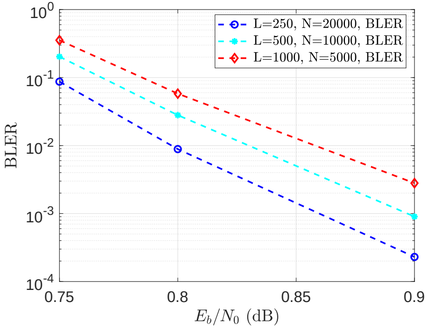

Figure 1: BLER performance of a (3,6)-regular SC-LDPC code for three different combinations of frame length L and number of frames N simulated, all with the same total number of simulated blocks ($LN = 5 \times 10^6$ blocks), for an AWGN channel with BPSK signaling.

- With increasing L, the *block error rate* (BLER) performance becomes worse, even though there are relatively few error propagation frames overall.
- This figure represents only a narrow range of SNRs, below the threshold of the underlying LDPC-BC, where decoding errors can propagate until the frame is terminated. For larger values of E_b/N_0 and/or W, SWD typically recovers from error propagation without terminating the frame.
- Under these conditions, BLER$\to 1$, as $L \to \infty$.

Motivation for CN Doped Codes

- **Observation 1**: The irregularities at the boundaries of a (J, K)-regular spatially coupled chain improve the performance of SC-LDPC codes (due to wave propagation) compared to the underlying (J, K)-regular LDPC-BC.
- **Observation 2**: When the code is terminated, any error propagation stops, beginning about $W/2$ blocks from the end of the frame, due to the reduced degree CNs.

	Error Performance (20000 frames, $L = 250$, $M = 2000$, $w = 2$, $W = 18$)	Index of error frame	Number of error bits in a frame	Start and end error blocks
Original (3,6)-regular SC-LDPC code	BER $= 5.979 \times 10^{-6}$ BLER $= 8.22 \times 10^{-5}$ $\#$ frame errors $=4$	Frame 2673	6	Blocks 144-147
		Frame 5924	6	Blocks 144-147
		Frame 18545	53800	Blocks 60-238
		Frame 19646	65697	Blocks 15-238

Construction of CN Doped Codes

Idea

Occasionally insert additional CNs into the protograph of a regular SC-LDPC code. This additional irregularity, referred to as *check node (CN) doping*, emulates termination but still allows continuous encoding and decoding. [1]

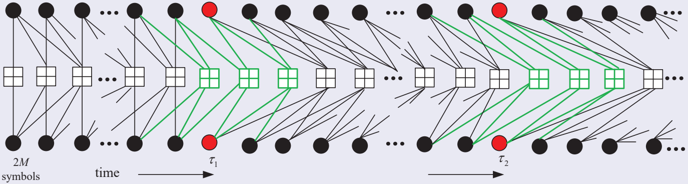

[1] CN doping is equivalent to *code extension*.

Construction of CN Doped Codes

Idea

Occasionally insert additional CNs into the protograph of a regular SC-LDPC code. This additional irregularity, referred to as *check node (CN) doping*, emulates termination but still allows continuous encoding and decoding. [1]

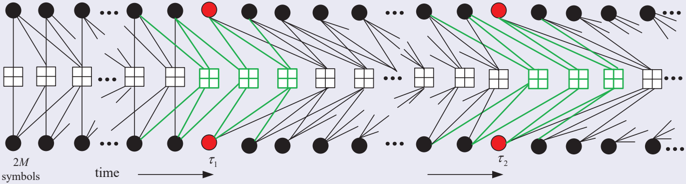

- The edges of the red VNs at time τ_j, representing the jth *doping point*, are connected to the CNs at times $\tau_j + j$, $\tau_j + j + 1$, and $\tau_j + j + 2$.

[1] CN doping is equivalent to *code extension*.

Construction of CN Doped Codes

Idea

Occasionally insert additional CNs into the protograph of a regular SC-LDPC code. This additional irregularity, referred to as *check node (CN) doping*, emulates termination but still allows continuous encoding and decoding. [1]

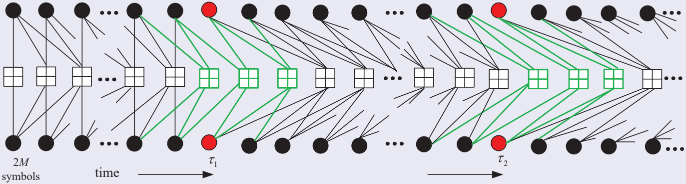

- The edges of the red VNs at time τ_j, representing the jth *doping point*, are connected to the CNs at times $\tau_j + j$, $\tau_j + j + 1$, and $\tau_j + j + 2$.
- The VNs between doping points (colored black) are coupled in the same way as the preceding red VN pair.

[1] CN doping is equivalent to *code extension*.

Construction of CN Doped Codes

Idea

Occasionally insert additional CNs into the protograph of a regular SC-LDPC code. This additional irregularity, referred to as *check node (CN) doping*, emulates termination but still allows continuous encoding and decoding. [1]

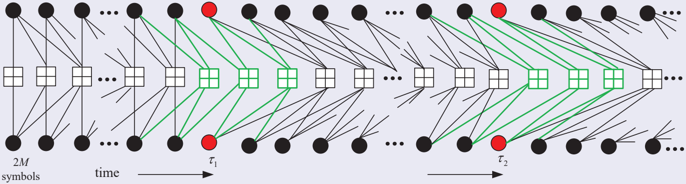

- The edges of the red VNs at time τ_j, representing the jth *doping point*, are connected to the CNs at times $\tau_j + j$, $\tau_j + j + 1$, and $\tau_j + j + 2$.
- The VNs between doping points (colored black) are coupled in the same way as the preceding red VN pair.
- Inserting doped CNs periodically into the coupled chain, i.e., *periodic CN doping*, results in the doping positions being *equally spaced* in the coupled chain. In this case, the doping positions (the red VNs) at times $t = \tau_1$ and τ_2 are fixed to known values and spaced s time units apart, i.e., $\tau_k = \tau_1 + (k-1)s$.

[1] CN doping is equivalent to *code extension*.

Construction of CN Doped Codes

The construction from the spatially coupled base matrix point of view:

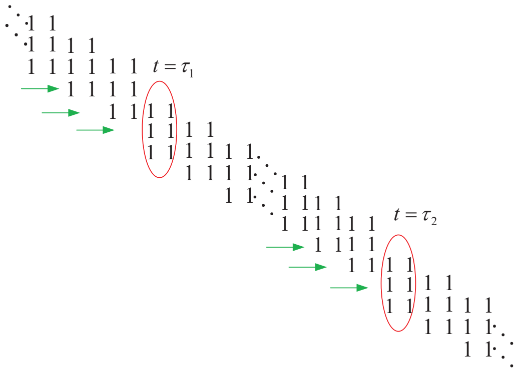

- The construction has the effect of inserting an additional CN at each doping point, resulting in three degree 4 CNs.

Construction of CN Doped Codes

The construction from the spatially coupled base matrix point of view:

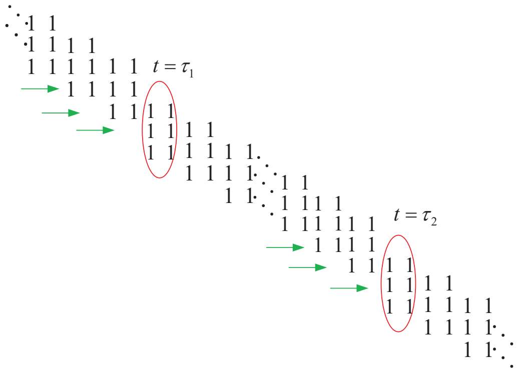

- The construction has the effect of inserting an additional CN at each doping point, resulting in three degree 4 CNs.
- This creates stronger "local" codes, thus facilitating the ability of a SWD to truncate error propagation, at the cost of a small rate loss.

Decoding of CN Doped Codes

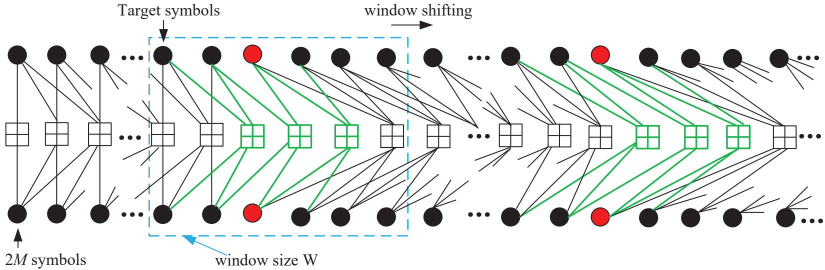

- For a window of size W, the block of $2M$ symbols at the earliest time (leftmost position in the window) is the target block.

Decoding of CN Doped Codes

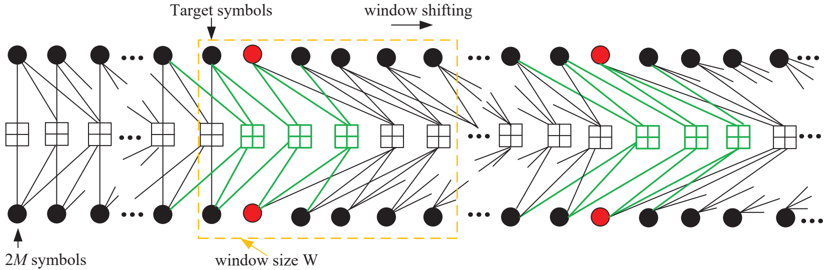

- For a window of size W, the block of $2M$ symbols at the earliest time (leftmost position in the window) is the target block.
- Normally, after a block of target symbols is decoded, the window (VNs and CNs) shifts by one time unit.

Decoding of CN Doped Codes

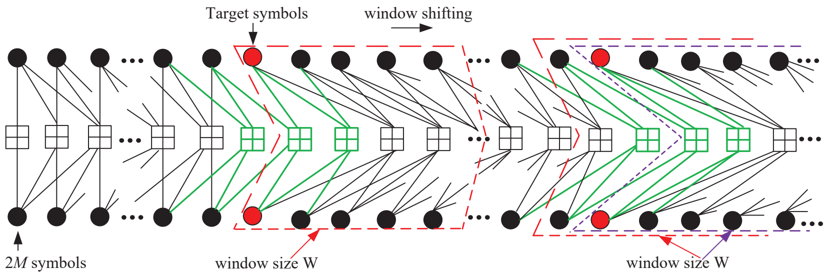

- For a window of size W, the block of $2M$ symbols at the earliest time (leftmost position in the window) is the target block.
- Normally, after a block of target symbols is decoded, the window (VNs and CNs) shifts by one time unit.
- When a doping point (red VN pair) becomes the target block, the window shifts by one VN time unit to include one new block of VNs and by two CN time units to include two new blocks of CNs, after which normal window shifting resumes.

Decoding of CN Doped Codes

The decoding from the spatially coupled base matrix point of view:

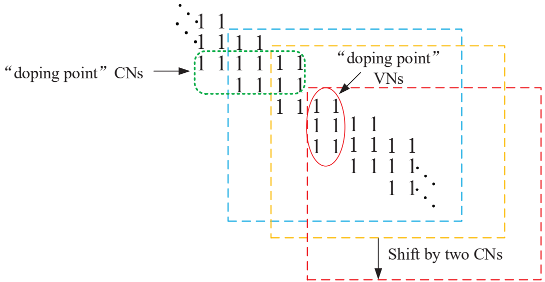

- Each time a doping point is reached, the window shifts down by two rows.

Numerical Results (effectiveness of code doping)

- In order to verify the effectiveness of code doping, the bit error rate (BER) distribution per block of a typical frame subject to error propagation in SWD of both doped and undoped (3,6)-regular SC-LDPC codes is shown.

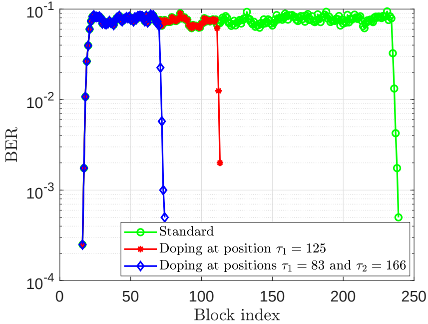

Figure 2: BER distribution per block of doped and undoped (3,6)-regular SC-LDPC codes with $M = 2000$, $W = 18$, and $L = 250$.

Numerical Results (effectiveness of code doping)

- In order to verify the effectiveness of code doping, the bit error rate (BER) distribution per block of a typical frame subject to error propagation in SWD of both doped and undoped (3,6)-regular SC-LDPC codes is shown.

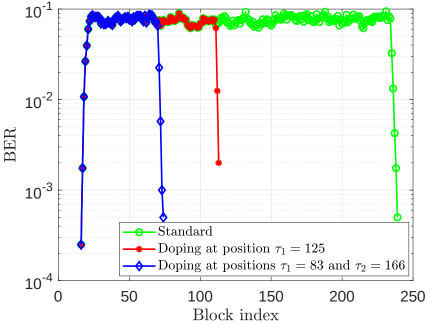

Figure 2: BER distribution per block of doped and undoped (3,6)-regular SC-LDPC codes with $M = 2000$, $W = 18$, and $L = 250$.

- We can clearly see that doping effectively truncates the error propagation and that adding more doped nodes truncates the error propagation earlier.

Numerical Results (performance comparison)

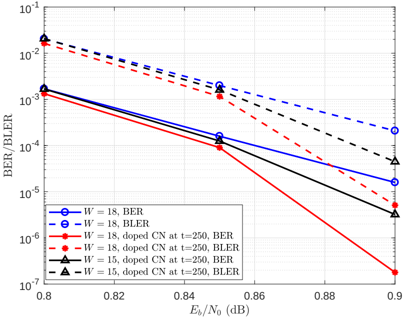

Figure 3: Performance comparison of doped and undoped (3,6)-regular SC-LDPC codes with $L = 500$, $W = 18$, and $W = 15$.

Numerical Results (performance comparison)

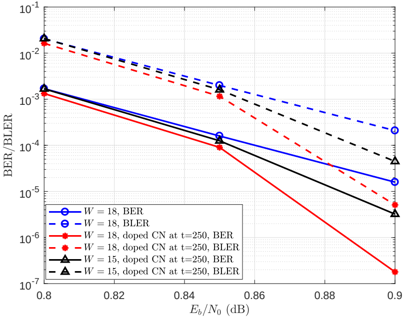

Figure 3: Performance comparison of doped and undoped (3,6)-regular SC-LDPC codes with $L = 500$, $W = 18$, and $W = 15$.

- The doped code gains up to two orders of magnitude in BER and more than one order of magnitude in BLER compared to the undoped code.
- The doped code with $W = 15$ provides almost an order of magnitude coding gain *plus* a 16% reduction in decoding latency compared to the undoped code with $W = 18$.

Rate Loss of CN Doping

- Let n_c' and n_v' denote the total number of CNs and the total number of VNs in CN doped SC-LDPC codes, respectively.

Rate Loss of CN Doping

- Let n'_{c} and n'_{v} denote the total number of CNs and the total number of VNs in CN doped SC-LDPC codes, respectively.
- The *design rate* of the CN doped SC-LDPC codes with frame length L and d doping positions is given by

$$R_L^{\mathrm{CN}} = 1 - \frac{n'_{\mathrm{c}}}{n'_{\mathrm{v}}} = 1 - \frac{(L+w+d)\, n_c}{L n_v} = 1 - \left(\frac{L+w+d}{L}\right)(1-R)\,,$$

where $R = 1 - n_{\mathrm{c}}/n_{\mathrm{v}}$ is the *design rate* of the uncoupled LDPC-BC protograph.

Rate Loss of CN Doping

- Let n'_{c} and n'_{v} denote the total number of CNs and the total number of VNs in CN doped SC-LDPC codes, respectively.
- The *design rate* of the CN doped SC-LDPC codes with frame length L and d doping positions is given by

$$R_L^{\mathrm{CN}} = 1 - \frac{n'_{\mathrm{c}}}{n'_{\mathrm{v}}} = 1 - \frac{(L + w + d)\, n_c}{L n_v} = 1 - \left(\frac{L + w + d}{L}\right)(1 - R)\,,$$

  where $R = 1 - n_{\mathrm{c}}/n_{\mathrm{v}}$ is the *design rate* of the uncoupled LDPC-BC protograph.
- Compared to the *design rate* $R_L = 1 - \left(\frac{L+w}{L}\right)(1 - R)$ of undoped SC-LDPC codes, we see that the design rate R_L^{CN} of CN doped SC-LDPC codes is smaller, i.e., CN doping results in some *rate loss*.

Rate Loss of CN Doping

- Let n'_{c} and n'_{v} denote the total number of CNs and the total number of VNs in CN doped SC-LDPC codes, respectively.
- The *design rate* of the CN doped SC-LDPC codes with frame length L and d doping positions is given by

$$R_L^{\mathrm{CN}} = 1 - \frac{n'_{\mathrm{c}}}{n'_{\mathrm{v}}} = 1 - \frac{(L + w + d)\, n_c}{L n_v} = 1 - \left(\frac{L + w + d}{L}\right)(1 - R)\,,$$

  where $R = 1 - n_{\mathrm{c}}/n_{\mathrm{v}}$ is the *design rate* of the uncoupled LDPC-BC protograph.
- Compared to the *design rate* $R_L = 1 - \left(\frac{L+w}{L}\right)(1 - R)$ of undoped SC-LDPC codes, we see that the design rate R_L^{CN} of CN doped SC-LDPC codes is smaller, i.e., CN doping results in some *rate loss*.
- *Termination* at the doping positions, which also truncates error propagation, would result in a larger rate loss.

Rate Loss of CN Doping

- Design rates of periodic CN doping for different values of d are calculated below.

  Example: Consider (3,6)-regular SC-LDPC codes with frame length $L = 1000$.

  Case 1: $d = 0$, $R_{1000} = 1 - \left(\frac{1000+2}{1000}\right)(1 - 0.5) = 0.499$.

  Case 2: $d = 1$, $R_{1000}^{\text{CN}} = 1 - \left(\frac{1000+2+1}{1000}\right)(1 - 0.5) = 0.4985$.
  For termination at $L = 500$, $R_{500} = 1 - \left(\frac{500+2}{500}\right)(1 - 0.5) = 0.498$.

  Case 3: $d = 3$, $R_{1000}^{\text{CN}} = 1 - \left(\frac{1000+2+3}{1000}\right)(1 - 0.5) = 0.4975$.
  For termination at $L = 250$, $R_{250} = 1 - \left(\frac{250+2}{250}\right)(1 - 0.5) = 0.496$.

Rate Loss of CN Doping

- Design rates of periodic CN doping for different values of d are calculated below.

  Example: Consider (3,6)-regular SC-LDPC codes with frame length $L = 1000$.

  Case 1: $d = 0$, $R_{1000} = 1 - \left(\frac{1000+2}{1000}\right)(1 - 0.5) = 0.499$.

  Case 2: $d = 1$, $R_{1000}^{\text{CN}} = 1 - \left(\frac{1000+2+1}{1000}\right)(1 - 0.5) = 0.4985$.
  For termination at $L = 500$, $R_{500} = 1 - \left(\frac{500+2}{500}\right)(1 - 0.5) = 0.498$.

  Case 3: $d = 3$, $R_{1000}^{\text{CN}} = 1 - \left(\frac{1000+2+3}{1000}\right)(1 - 0.5) = 0.4975$.
  For termination at $L = 250$, $R_{250} = 1 - \left(\frac{250+2}{250}\right)(1 - 0.5) = 0.496$.

- From these results, we see that, even though CN doping results in some rate loss, the rate loss of termination is greater. □

Construction of VN Doped Codes

Idea

Occasionally fix the value of VNs in the protograph to a known symbol (0 or 1). This process, referred to as *variable node (VN) doping*, results in stronger local codes at the doping positions and thus emulates termination, while still allowing continuous encoding and decoding.[2]

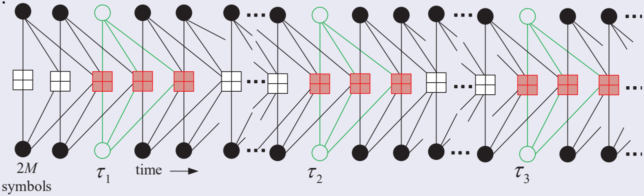

[2] VN doping is equivalent to *code shortening*.

Construction of VN Doped Codes

Idea

Occasionally fix the value of VNs in the protograph to a known symbol (0 or 1). This process, referred to as *variable node (VN) doping*, results in stronger local codes at the doping positions and thus emulates termination, while still allowing continuous encoding and decoding.[2]

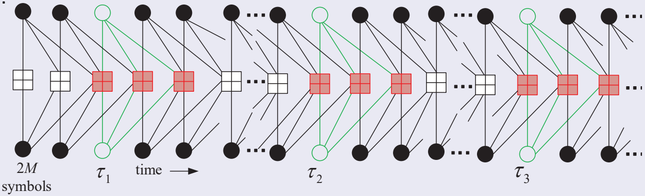

- During the decoding process we set the LLRs of the doped symbols to a large constant (positive or negative) value Γ. These known symbols have the effect of transmitting perfectly reliable information to their neighbor nodes, thus helping the decoder recover from error propagation.

[2]VN doping is equivalent to *code shortening*.

Construction of VN Doped Codes

Idea

Occasionally fix the value of VNs in the protograph to a known symbol (0 or 1). This process, referred to as *variable node (VN) doping*, results in stronger local codes at the doping positions and thus emulates termination, while still allowing continuous encoding and decoding.[2]

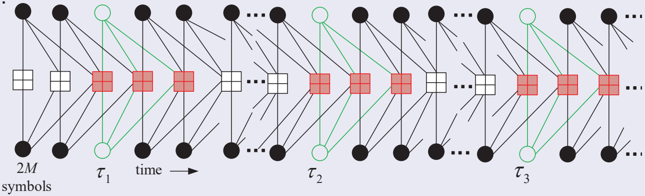

- During the decoding process we set the LLRs of the doped symbols to a large constant (positive or negative) value Γ. These known symbols have the effect of transmitting perfectly reliable information to their neighbor nodes, thus helping the decoder recover from error propagation.
- Inserting doped VNs periodically into the coupled chain, i.e., *periodic VN doping*, results in the doping positions being *equally spaced* in the coupled chain. In this case, the doping positions (the green VNs) at times $t = \tau_1$, τ_2, and τ_3 are fixed to known values and spaced s time units apart, i.e., $\tau_k = \tau_1 + (k-1)s$.

[2] VN doping is equivalent to *code shortening*.

Numerial Results (performance comparison)

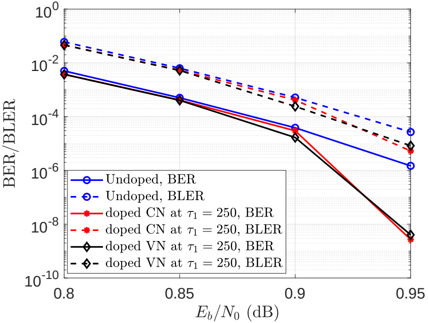

Figure 4: Performance comparison of CN doped, VN doped, and undoped (3,6)-regular SC-LDPC codes with $W = 12$.

Numerial Results (performance comparison)

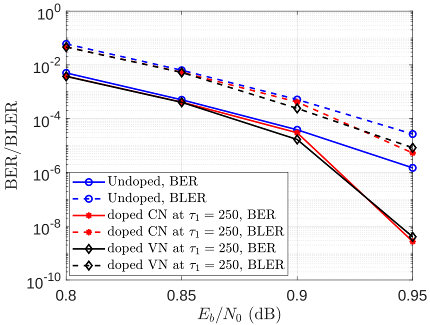

Figure 4: Performance comparison of CN doped, VN doped, and undoped (3,6)-regular SC-LDPC codes with $W = 12$.

- The *BER* and BLER performance of undoped (3,6)-regular SC-LDPC codes, VN doping, and CN doping is shown.
- Both VN doping and CN doping gain approximately two orders of magnitude in BER and one order of magnitude in BLER compared to the undoped code at these SNR values (below the threshold of the underlying LDPC-BC).

Rate Loss of VN Doping

- The *design rate* of VN doped SC-LDPC codes with frame length L and d doping positions is given by

$$R_L^{\mathrm{VN}} = 1 - \frac{n_c'}{n_v'} = 1 - \frac{(L+w)\, n_c}{(L-d)\, n_v} = 1 - [(L+w)/(L-d)]\,(1-R)\,.$$

Design rates of periodic VN doping for different values of d are calculated below.
Example (continued):

Case 1: $d = 0$, $R_{1000} = 1 - \left(\frac{1000+2}{1000}\right)(1-0.5) = 0.499$.
Case 2: $d = 1$, $R_{1000}^{\mathrm{VN}} = 1 - \left(\frac{1000+2}{1000-1}\right)(1-0.5) = 0.4985$.
For termination at $L = 500$, $R_{500} = 1 - \left(\frac{500+2}{500}\right)(1-0.5) = 0.498$.
Case 3: $d = 3$, $R_{1000}^{\mathrm{VN}} = 1 - \left(\frac{1000+2}{1000-3}\right)(1-0.5) = 0.4975$.
For termination at $L = 250$, $R_{250} = 1 - \left(\frac{250+2}{250}\right)(1-0.5) = 0.496$.

Rate Loss of VN Doping

- The *design rate* of VN doped SC-LDPC codes with frame length L and d doping positions is given by
$$R_L^{\mathrm{VN}} = 1 - \frac{n'_{\mathrm{c}}}{n'_{\mathrm{v}}} = 1 - \frac{(L+w)\,n_{\mathrm{c}}}{(L-d)\,n_{\mathrm{v}}} = 1 - [(L+w)/(L-d)]\,(1-R)\,.$$
Design rates of periodic VN doping for different values of d are calculated below.
Example (continued):

Case 1: $d = 0,\ R_{1000} = 1 - \left(\frac{1000+2}{1000}\right)(1-0.5) = 0.499.$

Case 2: $d = 1,\ R_{1000}^{\mathrm{VN}} = 1 - \left(\frac{1000+2}{1000-1}\right)(1-0.5) = 0.4985.$

For termination at $L = 500,\ R_{500} = 1 - \left(\frac{500+2}{500}\right)(1-0.5) = 0.498.$

Case 3: $d = 3,\ R_{1000}^{\mathrm{VN}} = 1 - \left(\frac{1000+2}{1000-3}\right)(1-0.5) = 0.4975.$

For termination at $L = 250,\ R_{250} = 1 - \left(\frac{250+2}{250}\right)(1-0.5) = 0.496.$

- Similar to the CN doping case, VN doping results in some rate loss, but the rate loss of termination is greater.

Rate Loss of VN Doping

- The *design rate* of VN doped SC-LDPC codes with frame length L and d doping positions is given by
$$R_L^{\mathrm{VN}} = 1 - \frac{n'_{\mathrm{c}}}{n'_{\mathrm{v}}} = 1 - \frac{(L+w)\,n_{\mathrm{c}}}{(L-d)\,n_{\mathrm{v}}} = 1 - [(L+w)/(L-d)]\,(1-R)\,.$$
Design rates of periodic VN doping for different values of d are calculated below.
Example (continued):

Case 1: $d = 0$, $R_{1000} = 1 - \left(\frac{1000+2}{1000}\right)(1-0.5) = 0.499.$
Case 2: $d = 1$, $R_{1000}^{\mathrm{VN}} = 1 - \left(\frac{1000+2}{1000-1}\right)(1-0.5) = 0.4985.$
For termination at $L = 500$, $R_{500} = 1 - \left(\frac{500+2}{500}\right)(1-0.5) = 0.498.$
Case 3: $d = 3$, $R_{1000}^{\mathrm{VN}} = 1 - \left(\frac{1000+2}{1000-3}\right)(1-0.5) = 0.4975.$
For termination at $L = 250$, $R_{250} = 1 - \left(\frac{250+2}{250}\right)(1-0.5) = 0.496.$

- Similar to the CN doping case, VN doping results in some rate loss, but the rate loss of termination is greater.
- Since in general $(L+w)\,/\,(L-d) > (L+w+d)\,/L$, the rate loss of VN doping is always greater than the rate loss of CN doping, but the difference is very slight for large values of L.

Adaptive VN Doping

- In contrast to periodic doping, adaptive doping inserts doping positions into the coupled chain on an "as needed" basis, depending on the average LLR magnitudes in some number of recently decoded target blocks.

Adaptive VN Doping

- In contrast to periodic doping, adaptive doping inserts doping positions into the coupled chain on an "as needed" basis, depending on the average LLR magnitudes in some number of recently decoded target blocks.
- Typically *unequally spaced* doping positions at times $t = \tau_1, \tau_2, \tau_3, \ldots$ are inserted into the coupled chain in response to requests from the decoder transmitted over a *noiseless binary feedback channel*.

Adaptive VN Doping

- In contrast to periodic doping, adaptive doping inserts doping positions into the coupled chain on an "as needed" basis, depending on the average LLR magnitudes in some number of recently decoded target blocks.
- Typically *unequally spaced* doping positions at times $t = \tau_1, \tau_2, \tau_3, \ldots$ are inserted into the coupled chain in response to requests from the decoder transmitted over a *noiseless binary feedback channel*.

After completing all the iterations necessary to decode the target block at time t, if the *average decoded LLR magnitude* $\mathcal{L}_t$ satisfies

$$\mathcal{L}_t \triangleq \frac{1}{2M} \sum_{i=0}^{2M-1} \left|\mathrm{LLR}_i^t\right| \leq \lambda, \tag{1}$$

where $\left|\mathrm{LLR}_i^t\right|$ is the LLR of the ith VN at time t, $i = 0, 1, \ldots, 2M-1$, and λ is some pre-determined *threshold*, we consider the target block at time t as *failed*.

Adaptive VN Doping

- In contrast to periodic doping, adaptive doping inserts doping positions into the coupled chain on an "as needed" basis, depending on the average LLR magnitudes in some number of recently decoded target blocks.
- Typically *unequally spaced* doping positions at times $t = \tau_1, \tau_2, \tau_3, \ldots$ are inserted into the coupled chain in response to requests from the decoder transmitted over a *noiseless binary feedback channel*.

After completing all the iterations necessary to decode the target block at time t, if the *average decoded LLR magnitude* $\mathcal{L}_t$ satisfies

$$\mathcal{L}_t \triangleq \frac{1}{2M} \sum_{i=0}^{2M-1} \left|\mathrm{LLR}_i^t\right| \leq \lambda, \quad (1)$$

where $\left|\mathrm{LLR}_i^t\right|$ is the LLR of the ith VN at time t, $i = 0, 1, \ldots, 2M-1$, and λ is some pre-determined *threshold*, we consider the target block at time t as *failed*.

- If we experience some preset number N_r of consecutive failed target blocks, a doping request is submitted and, assuming *instantaneous feedback*, the next block of VNs entering the far end of the window is assumed to be doped.

Numerical Results (effectiveness of adaptive doping)

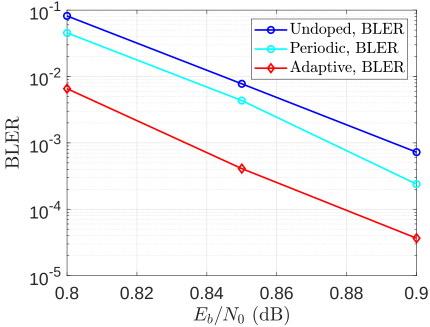

Figure 5: Performance comparison of undoped, periodically VN doped, and adaptively VN doped (3,6)-regular SC-LDPC codes with $M = 2000$, $W = 12$, $L = 1000$, and $R_{1000}^{\mathrm{VN}} \geq 0.4985$.

- The results confirm that, when low latency operation is desired at the lower SNRs typically used in practice, doping significantly improves the BLER performance, with adaptive doping outperforming periodic doping.

Numerical Results (effectiveness of adaptive doping)

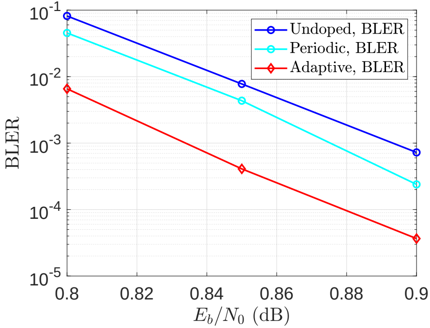

Figure 5: Performance comparison of undoped, periodically VN doped, and adaptively VN doped (3,6)-regular SC-LDPC codes with $M = 2000$, $W = 12$, $L = 1000$, and $R_{1000}^{\text{VN}} \geq 0.4985$.

- The results confirm that, when low latency operation is desired at the lower SNRs typically used in practice, doping significantly improves the BLER performance, with adaptive doping outperforming periodic doping.
- For adaptive doping, a limit was set such that the number of doping positions cannot exceed that of periodic doping.

Fractional VN Doping

Idea

Since each protograph node represents M VNs in the expanded graph, doping only a *fraction* δ, $0 \leq \delta \leq 1$, of the VNs at each doping position can reduce the rate loss.

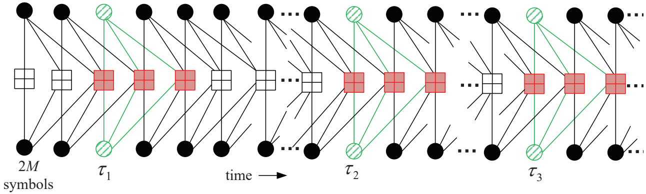

Fractional VN Doping

Idea

Since each protograph node represents M VNs in the expanded graph, doping only a *fraction* δ, $0 \leq \delta \leq 1$, of the VNs at each doping position can reduce the rate loss.

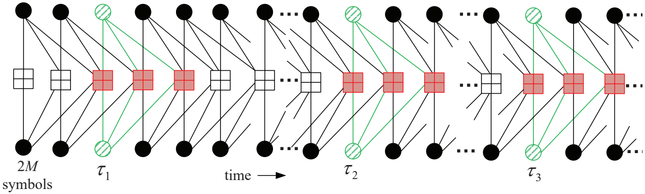

- The slashed circles represent the fractionally doped nodes and the solid circles represent undoped nodes.

Fractional VN Doping

Idea

Since each protograph node represents M VNs in the expanded graph, doping only a *fraction* δ, $0 \leq \delta \leq 1$, of the VNs at each doping position can reduce the rate loss.

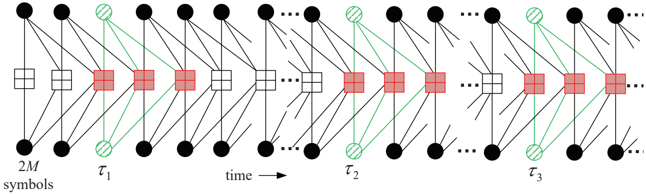

- The slashed circles represent the fractionally doped nodes and the solid circles represent undoped nodes.
- $\delta = 0$ corresponds to no doping and $\delta = 1$ corresponds to full doping.

Fractional VN Doping

Idea

Since each protograph node represents M VNs in the expanded graph, doping only a *fraction* δ, $0 \leq \delta \leq 1$, of the VNs at each doping position can reduce the rate loss.

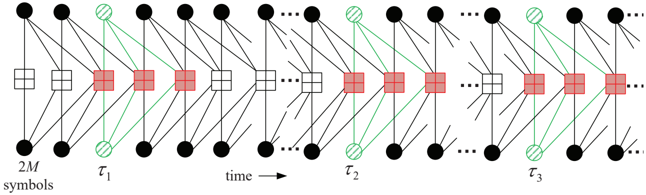

- The slashed circles represent the fractionally doped nodes and the solid circles represent undoped nodes.
- $\delta = 0$ corresponds to no doping and $\delta = 1$ corresponds to full doping.
- We divide the $2M$ symbols at each time unit into two sets: a *doped set* $\mathcal{D}$ and an *undoped set* $\bar{\mathcal{D}}$.

Fractional VN Doping

In fractional doping, let L_i^t, $1 \leq i \leq 2M$, denote the *channel LLR* used for decoding the ith bit at time unit t. Then we have

$$L_i^t = \begin{cases} \Gamma, & i \in \mathcal{D} \\ L_i^{t,\mathrm{ch}}, & i \in \bar{\mathcal{D}} \end{cases},$$

where $L_i^{t,\mathrm{ch}}$ denotes the *received channel LLR* of the ith bit at time unit t and $\Gamma = +10$ is chosen to denote the *known LLR value* corresponding to a doped bit 0.

Fractional VN Doping

In fractional doping, let L_i^t, $1 \leq i \leq 2M$, denote the *channel LLR* used for decoding the ith bit at time unit t. Then we have

$$L_i^t = \begin{cases} \Gamma, & i \in \mathcal{D} \\ L_i^{t,\mathrm{ch}}, & i \in \bar{\mathcal{D}} \end{cases},$$

where $L_i^{t,\mathrm{ch}}$ denotes the *received channel LLR* of the ith bit at time unit t and $\Gamma = +10$ is chosen to denote the *known LLR value* corresponding to a doped bit 0.

- This has the effect of assigning *certainty* to the doped bits during the decoding process.

Fractional VN Doping

- We considered two fractional doping patterns: *adjacent* doping and *periodic* doping, illustrated below for the case $\delta = 0.5$ (white circles represent doped bits and black circles represent undoped bits).

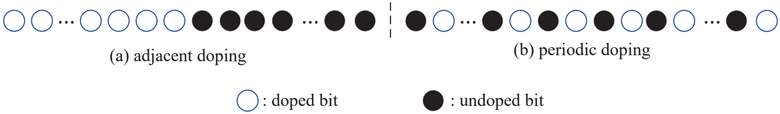

Fractional VN Doping

- We considered two fractional doping patterns: *adjacent* doping and *periodic* doping, illustrated below for the case $\delta = 0.5$ (white circles represent doped bits and black circles represent undoped bits).

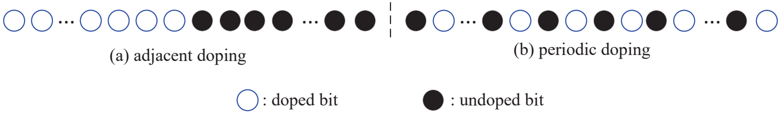

- At a doping position, for $\delta = 0.5$, adjacent doping is equivalent to doping all the VNs in one protograph node and no VNs in the other, whereas periodic doping spreads the doped VNs evenly over both protograph nodes.

Numerical Results (effectiveness of fractional doping)

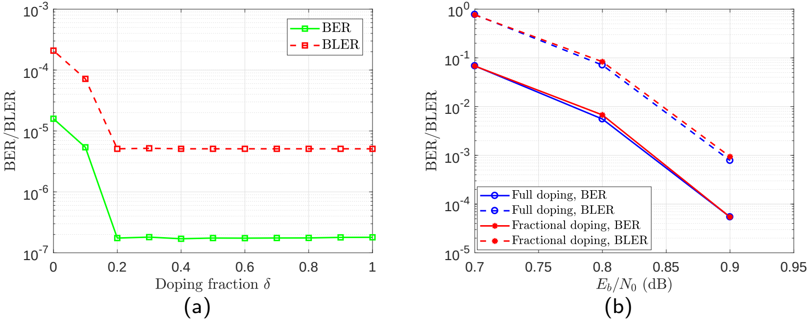

Figure 6: Performance of a fractionally doped (3,6)-regular SC-LDPC code for (a) $M = 2000$, $W = 18$, $L = 500$, and $E_b/N_0 = 0.9$ dB and (b) $M = 2000$, $W = 12$, $L = 250$, and $\delta = 0.5$.

- Consistent with the analytical results of [Sokolovskii 2021] for the BEC, even a small amount of fractional doping yields significant performance improvement.

Numerical Results (effectiveness of fractional doping)

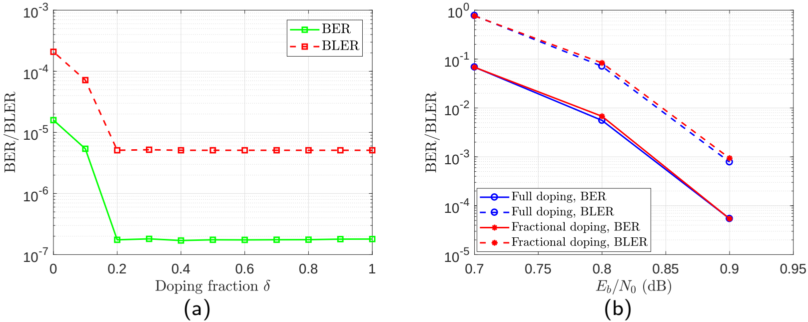

Figure 6: Performance of a fractionally doped (3,6)-regular SC-LDPC code for (a) $M = 2000$, $W = 18$, $L = 500$, and $E_b/N_0 = 0.9$ dB and (b) $M = 2000$, $W = 12$, $L = 250$, and $\delta = 0.5$.

- Consistent with the analytical results of [Sokolovskii 2021] for the BEC, even a small amount of fractional doping yields significant performance improvement.
- Fractional doping with $\delta = 0.5$ achieves essentially the same the BER and BLER performance as full doping, with only half the rate loss.

Systematic VN Doping

Motivation

- Designing a non-systematic encoder with doped code bits (or a systematic encoder with doped parity bits) in general leads to a highly complex encoding process.

Systematic VN Doping

Motivation

- Designing a non-systematic encoder with doped code bits (or a systematic encoder with doped parity bits) in general leads to a highly complex encoding process.
- In the decoding of LDPC codes, the decoding process results in an estimated code sequence, which must then be inverted according to the same highly complex encoding rule in order to recover the estimated information sequence.

Systematic VN Doping

Motivation

- Designing a non-systematic encoder with doped code bits (or a systematic encoder with doped parity bits) in general leads to a highly complex encoding process.
- In the decoding of LDPC codes, the decoding process results in an estimated code sequence, which must then be inverted according to the same highly complex encoding rule in order to recover the estimated information sequence.
- In the case of adaptive VN doping, these complex encoding and encoder inverse operations must be done "on the fly", whenever the feedback channel requests the insertion of doped bits into the encoded sequence.

Systematic VN Doping

Idea:

- If systematic encoding is used, doping can be done directly on the information sequence, prior to encoding, thus greatly simplifying the encoding process.

Systematic VN Doping

Idea:

- If systematic encoding is used, doping can be done directly on the information sequence, prior to encoding, thus greatly simplifying the encoding process.
- If only systematic bits are doped, the encoder inverse operation is trivial, since all the information bits appear unchanged as code bits in the encoded sequence, and thus the estimated information sequence can be determined directly from the estimated code sequence.

Systematic VN Doping

Idea:

- If systematic encoding is used, doping can be done directly on the information sequence, prior to encoding, thus greatly simplifying the encoding process.
- If only systematic bits are doped, the encoder inverse operation is trivial, since all the information bits appear unchanged as code bits in the encoded sequence, and thus the estimated information sequence can be determined directly from the estimated code sequence.
- Such a *systematic VN doping strategy* necessitates the use of fractional doping over a span of several positions in order to dope the same number of bits as full doping of all the protograph nodes at any one position.

Systematic VN Doping

To describe the procedure, we again use design rate $R = 1/2$ (3,6)-regular SC-LDPC codes as an example.

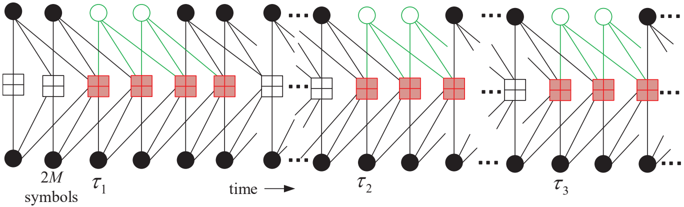

- The white circles represent the doped systematic protograph nodes.

Systematic VN Doping

To describe the procedure, we again use design rate $R = 1/2$ (3,6)-regular SC-LDPC codes as an example.

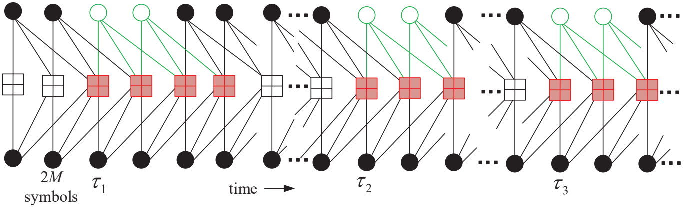

- The white circles represent the doped systematic protograph nodes.
- Assume that the upper protograph node at each position contains systematic bits only, while the lower protograph node contains parity bits only.

Systematic VN Doping

To describe the procedure, we again use design rate $R = 1/2$ (3,6)-regular SC-LDPC codes as an example.

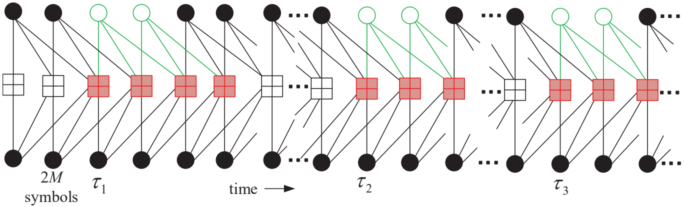

- The white circles represent the doped systematic protograph nodes.
- Assume that the upper protograph node at each position contains systematic bits only, while the lower protograph node contains parity bits only.
- In order to dope the same number of bits as full doping of a single position, systematic VN doping requires a *doping fraction* of $\delta \leq \mathrm{R} = 1/2$ symbols at each doped position and a *doping span* of $\sigma \geq 1/\mathrm{R} = 2$ consecutive positions such that $\sigma\delta = 1$, illustrated above for $\delta = R = 1/2$ and $\sigma = 1/R = 2$.

Systematic VN Doping

Now consider extending systematic VN doping to other rates,

- *Example 1*: (3,9)-regular SC-LDPC codes with design rate $R = 2/3$ and coupling width $w = 2$, derived from the 1×3 LDPC-BC base matrix $B = [3\ 3\ 3]$.

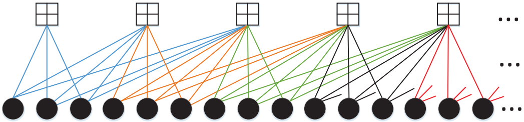

Systematic VN Doping

Now consider extending systematic VN doping to other rates,

- *Example 1*: (3,9)-regular SC-LDPC codes with design rate $R = 2/3$ and coupling width $w = 2$, derived from the 1×3 LDPC-BC base matrix $B = [3\ 3\ 3]$.

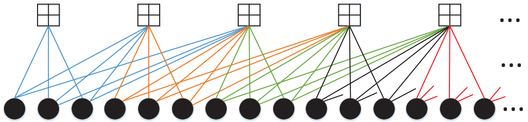

- There are three protograph nodes at each time unit: two nodes can be considered as *systematic nodes* and the other node as a *parity check node*.

Systematic VN Doping

- In this case, there are two options for doping the same number of bits as full doping of a single position:

  (i) doping span $\sigma = 2$ (see (a) below).
  Systematic doping operates over $\sigma = 2$ time units, where two systematic nodes are doped at time τ_1 and one systematic node is doped at time $\tau_1 + 1$.

  (ii) doping span $\sigma = 3$ (see (b) below).
  Systematic doping operates over $\sigma = 3$ time units, where one systematic node is doped at times $\tau_1, \tau_1 + 1$, and $\tau_1 + 2$.

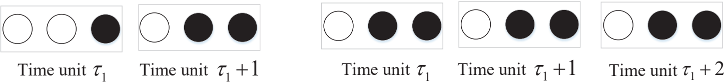

(a) doping span $\sigma = 2$

(b) doping span $\sigma = 3$

Systematic VN Doping

- *Example 2*: (4,6)-regular SC-LDPC codes with design rate $R = 1/3$ and coupling memory $w = 1$, derived from the 2×3 LDPC-BC base matrix

$$B = \begin{bmatrix} 2 & 2 & 2 \\ 2 & 2 & 2 \end{bmatrix}.$$

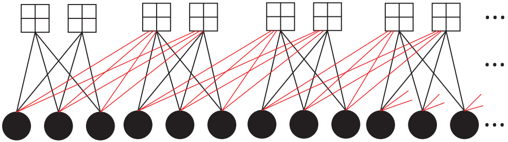

Systematic VN Doping

- *Example 2*: (4,6)-regular SC-LDPC codes with design rate $R = 1/3$ and coupling memory $w = 1$, derived from the 2×3 LDPC-BC base matrix

$$B = \begin{bmatrix} 2 & 2 & 2 \\ 2 & 2 & 2 \end{bmatrix}.$$

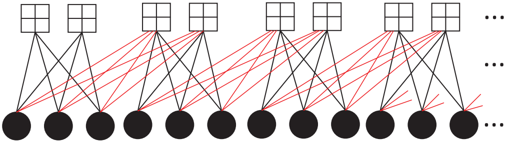

- There are three protograph nodes at each time unit: one node can be considered as a *systematic node* and the other two nodes as *parity check nodes*.

Systematic VN Doping

- *Example 2*: (4,6)-regular SC-LDPC codes with design rate $R = 1/3$ and coupling memory $w = 1$, derived from the 2×3 LDPC-BC base matrix

$$B = \begin{bmatrix} 2 & 2 & 2 \\ 2 & 2 & 2 \end{bmatrix}.$$

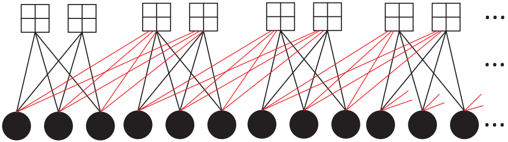

- There are three protograph nodes at each time unit: one node can be considered as a *systematic node* and the other two nodes as *parity check nodes*.
- In this case, since only one protograph node can be doped at each position, the doping option with $\sigma = 3$ must be used to dope the same number of bits as full doping of a single position.

Numerical Results (effectiveness of systematic doping)

- Performance comparison between full doping and systematic doping ($M = 1000$ and $L = 500$).

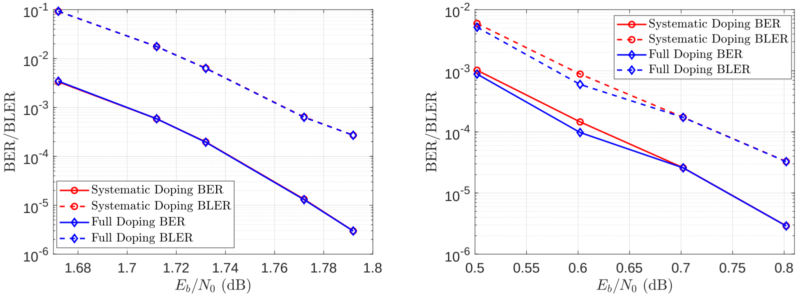

(a) (3,9)-regular SC-LDPC code with $W = 12$ (b) (4,6)-regular SC-LDPC code with $W = 8$

Figure 7: Performance comparison between full doping and systematic doping.

- The total number of doped VNs is $3\delta\sigma M = 3M$, both for systematic doping ($\delta = 1/3, \sigma = 3$) and full doping ($\delta = 1, \sigma = 1$).

Numerical Results (effectiveness of systematic doping)

- Performance comparison between full doping and systematic doping ($M = 1000$ and $L = 500$).

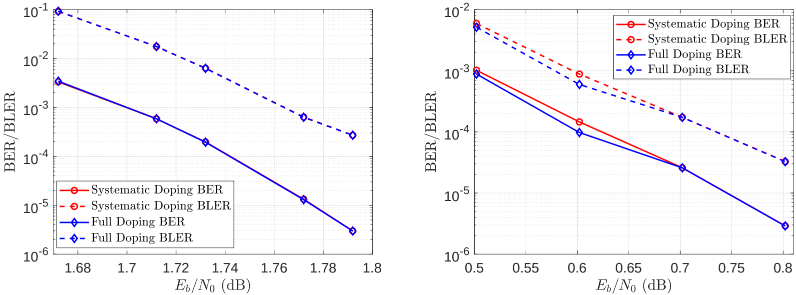

(a) (3,9)-regular SC-LDPC code with $W = 12$ (b) (4,6)-regular SC-LDPC code with $W = 8$

Figure 7: Performance comparison between full doping and systematic doping.

- The total number of doped VNs is $3\delta\sigma M = 3M$, both for systematic doping ($\delta = 1/3, \sigma = 3$) and full doping ($\delta = 1, \sigma = 1$).
- Systematic doping, which covers $\sigma = 3$ positions, achieves essentially the same BER and BLER performance as full doping of a single position, which involves a much more complex encoding process.

1. Introduction
2. Sliding Window Decoding (SWD) of LDPC Convolutional Codes
3. Decoder Error Propagation in SWD of LDPC Convolutional Codes
4. Check Node (CN) Doping
5. Variable Node (VN) Doping
6. Adaptive, Fractional, and Systematic VN Doping
7. **Summary**

Summary

- We investigated the decoder error propagation problem associated with SWD of SC-LDPC codes, which can cause significant performance degradation for large frame length applications, and we noted the difficulty of using conventional computer simulation methods to assess the severity of the problem.

Summary

- We investigated the decoder error propagation problem associated with SWD of SC-LDPC codes, which can cause significant performance degradation for large frame length applications, and we noted the difficulty of using conventional computer simulation methods to assess the severity of the problem.
- To combat this problem, we presented *check node (CN) doping* and *variable node (VN) doping* techniques for improving decoder performance and described how the performance can be further improved by using an adaptive approach that depends on the availability of a noiseless binary feedback channel.

Summary

- We investigated the decoder error propagation problem associated with SWD of SC-LDPC codes, which can cause significant performance degradation for large frame length applications, and we noted the difficulty of using conventional computer simulation methods to assess the severity of the problem.
- To combat this problem, we presented *check node (CN) doping* and *variable node (VN) doping* techniques for improving decoder performance and described how the performance can be further improved by using an adaptive approach that depends on the availability of a noiseless binary feedback channel.
- Code doping effectively allows us to mitigate the effects of decoder error propagation without frequently terminating encoding, thus facilitating streaming transmission, while also resulting in less rate loss than termination.

Summary

- We investigated the decoder error propagation problem associated with SWD of SC-LDPC codes, which can cause significant performance degradation for large frame length applications, and we noted the difficulty of using conventional computer simulation methods to assess the severity of the problem.
- To combat this problem, we presented *check node (CN) doping* and *variable node (VN) doping* techniques for improving decoder performance and described how the performance can be further improved by using an adaptive approach that depends on the availability of a noiseless binary feedback channel.
- Code doping effectively allows us to mitigate the effects of decoder error propagation without frequently terminating encoding, thus facilitating streaming transmission, while also resulting in less rate loss than termination.
- We showed how the encoding problem for VN doping can be greatly simplified by employing *systematic encoding* and *fractional doping* to dope only systematic bits, with little or no performance loss.

Summary

- We investigated the decoder error propagation problem associated with SWD of SC-LDPC codes, which can cause significant performance degradation for large frame length applications, and we noted the difficulty of using conventional computer simulation methods to assess the severity of the problem.
- To combat this problem, we presented *check node (CN) doping* and *variable node (VN) doping* techniques for improving decoder performance and described how the performance can be further improved by using an adaptive approach that depends on the availability of a noiseless binary feedback channel.
- Code doping effectively allows us to mitigate the effects of decoder error propagation without frequently terminating encoding, thus facilitating streaming transmission, while also resulting in less rate loss than termination.
- We showed how the encoding problem for VN doping can be greatly simplified by employing *systematic encoding* and *fractional doping* to dope only systematic bits, with little or no performance loss.
- Systematic VN doping of SC-LDPC codes with SWD represents a practical solution to achieve near capacity performance with limited decoding latency.